Brief Papers

On-Board Calibration of Spark Timing by Extremum Seeking for Flex-Fuel Engines

Erik Hellström, Donghoon Lee, Li Jiang, Anna G. Stefanopoulou, and Hakan Yilmaz

***Abstract*— An extremum-seeking controller is developed to cope with the calibration complexity for modern internal combustion engines capable of operating with different blends of ethanol and gasoline. The optimization scheme adapts the spark timing such that the fuel efficiency, estimated from in-cylinder pressure data, is maximized on-board a vehicle when driving with small load variations. Experiments, performed in a four-cylinder 2 L engine, demonstrate that the developed controller successfully manages to operate the engine close to the maximum fuel efficiency for different fuel blends, even under mild transient load conditions.**

***Index Terms*— Automotive control, extremum-seeking control, flex-fuel engines, spark ignition control.**

I. Introduction

VARIOUS advanced automotive technologies, such as direct-injection (DI), turbocharging (TC), and variable valve timing (VVT) have been integrated into gasoline spark ignited (SI) engines to increase their fuel efficiency while meeting emission standards and driveability requirements [1]–[3]. These degrees of freedom increase the complexity of the control design and the calibration. For engines capable of operating on different fuels (flex-fuel engines), such as gasoline-ethanol blends, the complexity increases even further due to the need for different calibration maps for different fuels. Most of the current engine controls in production are implemented based on maps with values calibrated off-line for various operating conditions using data from experiments performed in dynamometer facilities. To reduce the large calibration effort, we present a method for engine calibration for a flex-fuel TC SI DI engine by employing an extremum-seeking (ES) controller using in-cylinder pressure sensing to calibrate spark timing for on-board maximization of fuel efficiency. The controller structure is shown in Fig. 1.

The ES controller is evaluated in experiments on a flex-fuel SI DI engine equipped with TC and VVT. A simulation model is used for the development and tuning of the ES controller. The final ES controller, however, does not depend on any explicit mathematical models. The simulation model was presented in [4] and extended earlier models, in [5], [6], of the engine air path by modeling the combustion variability, which is important for capturing the effects of VVT settings that give high levels of internally recirculated exhaust gas affecting the fuel efficiency. In this paper, the experimental results show that the controller successfully converges to the optimum spark in approximately 20 s for a fixed load command. For transient load commands convergence is obtained if the load command, varying as a sinusoid, is slower than 0.1 Hz.

In the next section, a background on ES is given with particular attention to automotive applications. The ES controller is presented in Section III and the experimental evaluation is given in Section IV. Conclusions from the work are drawn in the final section.

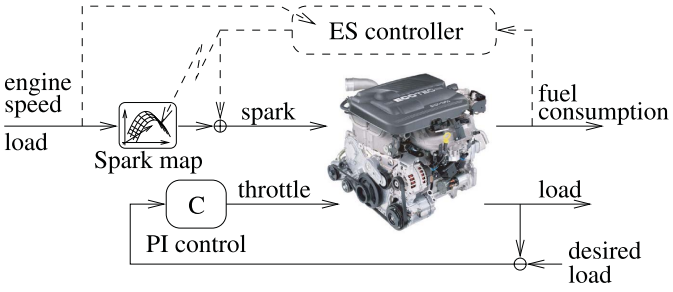

Fig. 1. Structure of the on-board calibration scheme. The ES controller (dashed lines) is added on to the spark control system, which typically is based on maps determined during the engine development, for on-board calibration of the spark timing for maximizing the fuel efficiency.

II. Background

The spark timing influences the torque output, the efficiency of the combustion, the produced emissions, and the engine knock. In most production engines, the control of the spark timing is currently open-loop and based on maps, feedback is only used for knock mitigation. The maps are calibrated in test rigs during the development of the engine in a simple but time-consuming process. For each point in the maps, the timing is tuned for some goals and then stored. The maps are typically a function of engine speed and load with compensations for ambient temperature, coolant temperature, and so forth. Such off-line calibration was automated in [7] utilizing ES methods.

The focus in this paper is on flex-fuel engines, where the fuel composition adds another dimension thereby increasing the development time with the traditional map-based approach. The approach here, shown in Fig. 1, is therefore to, instead, use

Manuscript received March 6, 2012; revised November 6, 2012; accepted December 17, 2012. Manuscript received in final form December 19, 2012. Date of publication January 9, 2013; date of current version October 15, 2013. This work was supported in part by the Department of Energy and Robert Bosch LLC. Recommended by Associate Editor S. M. Savaresi.

E. Hellström, D. Lee, and A. Stefanopoulou are with the Department of Mechanical Engineering, University of Michigan, Ann Arbor, MI 48109 USA (e-mail: erikhe@umich.edu; huni@umich.edu; annastef@umich.edu).

L. Jiang and H. Yilmaz are with Robert Bosch LLC, Farmington Hills, MI 48331 USA (e-mail: Li.Jiang@us.bosch.com; Hakan.Yilmaz@us.bosch.com).

Color versions of one or more of the figures in this paper are available online at http://ieeexplore.ieee.org.

Digital Object Identifier 10.1109/TCST.2012.2236093

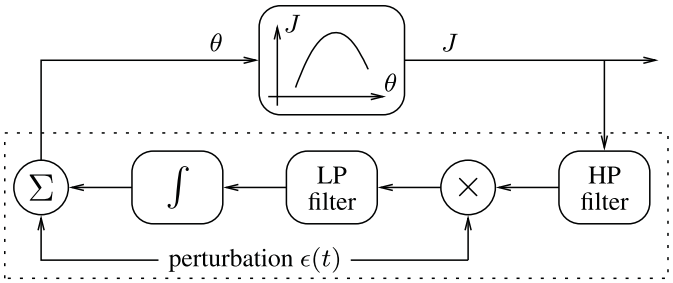

Fig. 2. On-board calibration of spark timing is based on perturbation-based ES [12]. A small perturbation, $\epsilon(t)$, is added to the input, θ, of the system. The output, J, is passed through a high-pass (HP) filter and multiplied with $\epsilon(t)$. The mean component, after the low-pass (LP) filter, is proportional to the slope of the criterion, $J'(\theta)$, and drives the integrator.

feedback from in-cylinder pressure sensors in an ES controller for calibrating the spark ignition timing on-board such that the fuel efficiency is maximized. Cylinder-pressure sensing is not typically available in production engines today but is an emerging technology for closed-loop combustion control [8].

ES control is concerned with finding the inputs to a process such that a function of the outputs, the objective, is at an extremum value [9]. The exact location of the extremum is unknown and the goal for the controller is to locate the extremum on-line. An early presentation of ES was given by Draper and Li [10] where several methods were proposed. The methods were classified as either being based on determining the slope of the input-to-output map, and driving the slope to zero, or based on peak-holding, where the control is based on the difference between the current output and the previous largest value of the output. In the first class of methods, the slope is obtained directly by differentiation of the output or by adding a small sinusoidal perturbation signal to the input. The peak-holding method was applied in [10] for maximizing engine torque with a constant fuel rate, which is equivalent to maximizing the efficiency, by controlling either ignition timing or intake manifold pressure. Experiments with a CFR engine[1] were performed at constant speed and fueling where the torque was obtained from the dynamometer output. The method in the present work is based on the scheme proposed by Blackman [12], shown in Fig. 2. Controllers utilizing square-wave perturbations in the spark timing for maximizing torque, estimated based on engine speed fluctuations, were developed in [13]. The stability of ES, when the objective is a static function of the equilibria of a nonlinear system controlled with a locally stabilizing control law, is proved in [14]. For a nonlinear dynamic system, the stability proof requires that the dynamics of the ES controller is on a slower time scale than the dynamics of the plant equilibria.

Methods based on nonlinear programming have been proposed in [15] and applied for calibrating valve and spark timings for an engine in [7]. Non-parametric approaches, which include all methods mentioned so far, using sinusoidal perturbation have been the most widely used for applications of ES [9, Ch. 1]. However, parametric approaches, where the objective function is estimated, have also been proposed [16], [17] and applied for ignition tuning in [18]–[20].

The method chosen in this paper, based on Fig. 2, is non-parametric where square-wave perturbations in spark timing are used. The objective of the controller is to maximize fuel efficiency, which is estimated from in-cylinder pressure sensor data. Compared to earlier applications, the novelties of the problem formulation are that the optimum operation is to be obtained for different fuel blends and during transient load conditions.

III. ES Controller

The spark ignition timing, θ_s, is the manipulated variable and the objective is to maximize fuel efficiency, which is obtained by minimizing the net specific fuel consumption (NSFC) defined by

$$\text{NSFC} = \frac{m_i}{W_n} \tag{1}$$

where m_i is the known injected fuel amount each engine cycle and W_n is the net indicated work per cycle computed from the measured cylinder pressure p and known volume V. The optimum spark timing, which achieves minimum NSFC, is denoted by θ_s^*.

The net work W_n is, as said, determined from the cylinder pressure. to illustrate the problem at hand, note that the net work W_n is the difference between the gross work W_g and the pumping work W_p, which is approximated by

$$W_n = W_g - W_p = m_i q_{lhv} \eta - (p_{em} - p_{im}) V_d \tag{2}$$

where q_{lhv} is the lower heating value of the fuel, η is the indicated gross efficiency, (p_{em}, p_{im}) are the exhaust and intake manifold pressures, respectively, and V_d is the displacement. The desired operating condition, engine speed and load, affects the fuel amount m_i and the pressures (p_{em}, p_{im}). The heating value is a property of the fuel and varies substantially for gasoline-ethanol blends, q_{lhv} is, approximately, 27 J/mg for ethanol and 44 J/mg for gasoline [11, App. D]. The efficiency η is a complex function of operating variables and engine design, for a given engine it is mainly determined by spark timing, air-fuel-ratio, and engine speed [11, Ch. 9]. All the influencing factors coupled with, e.g., component aging and varying ambient conditions lead to an increased off-line calibration effort for optimum operation. As mentioned earlier, the aim here is to avoid the extra dimension of fuel composition in the calibration maps and, instead, do the adaptation on-line. The characteristics of the objective, which is optimized on-line, are illustrated in Fig. 3. The figure shows data on the influence of engine speed and load on the curvature and the location of the minimum of the curve for NSFC versus spark timing θ_s. The value of the NSFC is normalized with its minimum value, in order to facilitate the comparison, and the spark timing is given in crank angle degrees (cad) after top dead center (TDC). So if the spark timing is negative, it should be understood that it occurs before TDC. The minimum NSFC occurs with θ_s in between -21 and -25 cad and the curves tend to be more flat at lower loads and speeds. When the spark timing retards,

[1]A standardized single-cylinder engine developed in 1931 for determining the octane rating of fuels [11, p. 471].

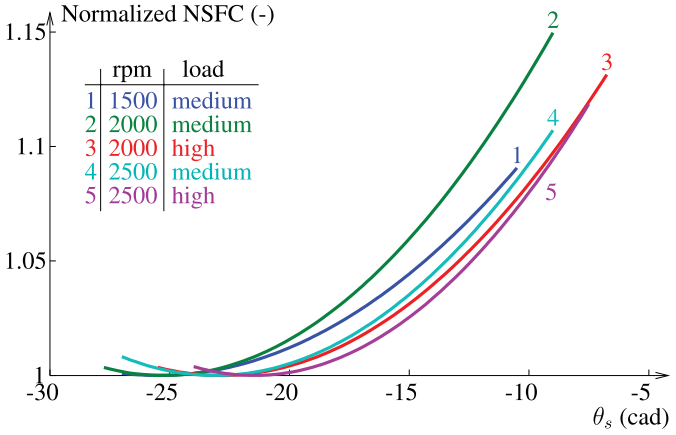

Fig. 3. Curves for normalized NSFC versus spark timing θ_s fitted to measurements at varying speed and load with E85 fuel. The curvature and the location of the minimum vary for the different conditions.

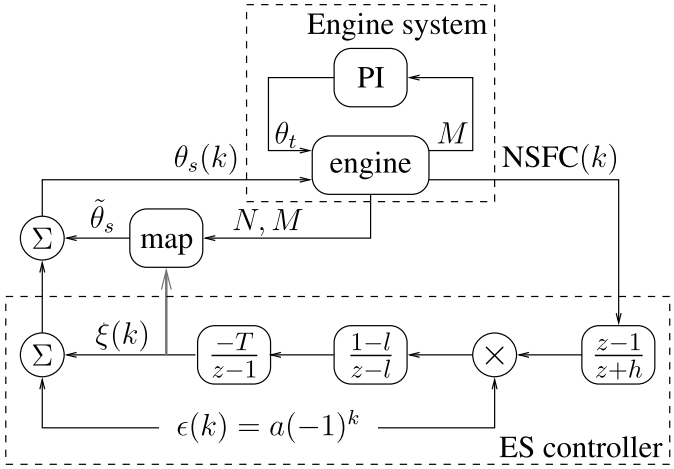

Fig. 4. Discrete perturbation-based ES control for spark timing, θ_s. The ES controller perturbs the spark angle as means to find the minimum NSFC while the engine load is regulated by PI-control of the throttle angle, θ_t.

meaning that the ignition occurs later, the NSFC increases significantly for all cases.

Because of the described complexity and uncertainties of the combustion process, an adaptive optimization scheme that does not rely on a plant model, such as ES, is a competitive approach. The time for convergence of such schemes is of importance, especially for passenger vehicles that typically operate in transient conditions. However, cruising conditions are fairly stationary and frequently visited for durations that should be sufficient for adaptation. Hence, the approach here, shown in Fig. 1, is to use ES to adapt the spark timing for maximum fuel efficiency in such conditions. The desired engine load is regulated with a PI-controller to set points while the pre-calibrated maps are used for spark and valve timings. When the ES algorithm has converged, the result is used to update the closest point in the spark timing map. An adaptation in one operating point can also be utilized to adapt neighboring points, a technique used in [13]. Even if the adaptation is not performed for the entire operating space, the gain of maximizing fuel efficiency in frequently visited conditions could be substantial.

The optimization problem is thus to find the optimum spark timing, θ_s^*, given by

$$\theta_s^* = \arg\min_{\theta_s} \left\{ n_c m_i \left(\sum_{k=1}^{n_c} \oint p_k \, dV \right)^{-1} \right\} \qquad \text{(OP)}$$

where n_c is the number of cylinders, p_k denotes the measured pressure in cylinder k, and the integral is taken over the four-stroke cycle of two engine revolutions. The problem (OP) is solved on-line with an ES controller. The ES controller searches for the solution to (OP) by adjusting the spark θ_s based on the observed response in the fuel consumption, measured by the NSFC, when perturbing θ_s. Although it is straightforward, a cylinder-individual approach to (OP) was not taken since the variations between cylinders in the experimental setup were small. Note also that such an approach would require one map for each cylinder. The operation of the ES controller in Fig. 2 is roughly described as follows. the high-pass filter removes the average value of the objective function. The signal, after multiplication with the perturbation and low-pass filtering, is approximately proportional to the slope of the objective. This signal drives the integrator, which will push $\theta_s(k)$ toward the minimum of the objective. In the following section, this controller is described in more detail.

The objective function in (OP) directly reflects the fuel efficiency of the engine. A principle that relates the fuel efficiency to a set point, which is independent of the fuel properties and can be regulated by feedback control, could be used for developing a simplified controller. For example if the combustion phasing corresponding to θ_s^* could be approximated constant and calibrated off-line.

A. Controller Structure and Parametrization

The problem (OP) is discrete since the criterion is defined by one value per one complete engine cycle of four strokes for all cylinders. Moreover the control variable, the spark timing, is scheduled once in each cycle. The discrete ES controller for this problem, based on the continuous controller in Fig. 2, is shown in Fig. 4. The sample time is denoted by T and chosen so that the engine and the load controller, denoted by Engine system in Fig. 4, can be approximated as a static nonlinearity for the NSFC as a function of θ_s, as mentioned above in Section II, the ES control is stable and converges when the objective is a static map with an extremum value [14]. The value of the sample time is based on simulations, using the mean value model in [4] of the engine, showing that the settling time is less than 30 cycles for typical steps in the commanded load. The sample time is 30 engine cycles, thus

$$T = 30 \cdot \frac{120}{N} \quad \text{(s)} \qquad (3)$$

where N is the engine speed in revolutions per minute. The filters are chosen to be of first order and are parameterized by (h, l). The filters are tuned, using the same simulation model, for convergence performance. At 2000 rpm, the parameters are chosen as $h = 35$ and $l = 13$. An exhaustive search for the best parameter set was not performed, other tuning parameters can

TABLE I
SPECIFICATIONS FOR THE OPTIMIZED FFV ENGINE

Description	Value
Cylinder volume	551.0 mm^3
Cylinder displacement volume	500.0 mm^3
Cylinder clearance volume	51.0 mm^3
Compression ratio	10.8:1
Valve timing (all angles at 0.25 mm lift)	
Intake valve open duration	264 cad
Exhaust valve open duration	221 cad

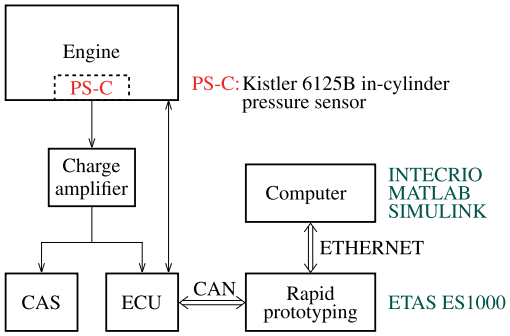

Fig. 5. Experimental setup at the engine dynamometer.

work or even outperform the ones selected. The perturbation, ϵ, is chosen as

$$\epsilon(k) = a(-1)^k \tag{4}$$

where k is the iteration number. The amplitude, a, is chosen to 1.5 crank angle degrees (cad) as a compromise between good signal-to-noise ratio for the NSFC and an acceptable level of torque variations.

IV. EXPERIMENTAL RESULT

A SI DI 4-cylinder 2 L flex-fuel engine with TC and VVT was used in the experiments, the specifications of the engine are summarized in Table I. The experimental setup at the engine dynamometer, illustrated in Fig. 5, consists of the Bosch MED17.3.2 ECU (electronic control unit) for engine controls, the ETAS ES1000 VME for rapid prototyping, and the A&D Redline CAS (combustion analysis system) for real-time combustion analysis. The ETAS ES1000 VME rapid prototyping system communicates with the ECU and a computer via CAN (controller-area network) and Ethernet, respectively. The outputs from cylinder pressure sensors, Kistler 6125B installed in each cylinder, are converted into voltage signals by an external charge amplifier. The voltage signals are read by the Bosch ECU and the A&D CAS. The CAS is used for off-line analysis of combustion features whereas the ECU acquires the cylinder pressure measurements and conducts real-time calculation of the net indicated work W_n as well as other key combustion features, such as the crank angle at which 50% of the total heat release has occurred, CA50. The ES controller for spark was implemented through the rapid prototyping environment made up of MATLAB/Simulink together with the ETAS hardware and the INTECRIO software. Engine load is, in the following, reported in units of percent relative load (%RL). In SI engines, RL is defined as the actual cylinder air charge divided by the maximum possible air charge when naturally aspirated (without TC). Furthermore, all crank angles are given in crank angle degrees (cad) after top dead center of the combustion. This means, e.g., that a typical spark timing θ_s is negative while the combustion phasing CA50 is positive.

A. Overview of the Experiments

The ES controller was tested for two engine speeds, N, of 1500 and 2000 rpm. The fuels used were E70, meaning a blend of 70% ethanol and 30% gasoline by volume, and E85. These blends are representative of what are typically available at the pump, which depends on the season. Fuels of high ethanol content are also preferred due to their higher antiknock quality, hence a lower risk for potentially damaging knock while trying the ES algorithm. The nominal RL was 50% at 1500 rpm and the nominal RL at 2000 rpm was 50% or 70%. For each of the nominal speed and load conditions, the optimum spark timings, θ_s^*, were determined through a conventional calibration using a design of experiment approach. The main benefit of using ES is that it can reduce the calibration effort and adapt for varying conditions, such as the current fuel blend in the vehicle tank. The calibration here was done in order to enable an evaluation of the ES controller performance with respect to a known optimum. The values in the ECU map, $\tilde{\theta}_s$ in Fig. 4, are modified from θ_s^* so that

$$\tilde{\theta}_s = \theta_s^* - \Delta \tag{5}$$

where the size of the disturbance, Δ, was -6, -9, or -12 cad. These values of Δ retard the combustion and decrease the fuel efficiency according to the trends in Fig. 3. Negative values of Δ were chosen to ensure safe operation without excessively knocking combustion. Note also that the calibrated value, θ_s^*, is a function of load and speed. From the block diagram in Fig. 4 and (5), we have that the deviation from the known optimum is

$$\theta_s - \theta_s^* = \xi - \Delta + \epsilon. \tag{6}$$

Hence, the ES controller state ξ, which is the required correction to the map, should ideally converge to Δ, $\xi \to \Delta$.

In the first set of experiments, the commanded load was a constant value of RL. To investigate the controller performance in transient conditions, the commanded RL was a sinusoidal function of time in a second set of experiments. The choice to vary RL while keeping engine speed constant is based on the fact that the optimum spark timing is more sensitive to load than to speed. Slow sinusoidal load variations are chosen as being representative of, e.g., the slow variations induced by the changing elevation along a vehicle's route. Table II summarizes the engine operating conditions for the tests at fixed loads. For the transient experiments, the nominal engine speed was 2000 rpm and the nominal relative load RL was 50%. The commanded relative load was

$$\mathrm{RL}(t) = 50 + A_L \sin\frac{2\pi t}{T_L} \quad (\%) \tag{7}$$

where the amplitude, A_L, and the period, T_L, were varied as given in Table III.

TABLE II
OPERATING CONDITIONS FOR THE FIXED LOAD EXPERIMENTS

Engine Speed N (rpm)	Relative Load RL (%)	Spark Timing Offset Δ (cad)	Fuel (E%)
1500	50	−6, −9, −12	E70
2000	50	−6, −9, −12	E85
	70	−6, −9, −12	E70

TABLE III
OPERATING CONDITIONS FOR THE TRANSIENT EXPERIMENTS AT $N = 2000$ rpm AND RL = 50%

Load Amplitude A_L (%)	Load Period T_L (s)	Fuel (E%)
3	100, 20, 10, 6.7	E85
5	100, 20, 10	E85

At the start of each experiment, the ES controller state, $\xi(k)$ in Fig. 4, is initialized to zero and the value in the ECU map, $\tilde{\theta}_s$ in Fig. 4, is set according to (5). The ES control algorithm is enabled when the engine operating conditions are inside the target sets of engine speed and load, defined as intervals around the nominal values. The criterion for convergence in the experiments is that the state $\xi(k)$ is inside an interval for 200 cycles. The number of cycles and the intervals were determined heuristically during preliminary experiments. In order to study the repeatability, during each experiment, the commanded engine load was perturbed outside the target area for a short while after the ES controller has converged. This causes the ES controller to be disabled and then re-enabled.

B. Fixed Load Conditions

Two sets of representative results from the dynamometer tests under fixed load are shown in Figs. 6 and 8. Fig. 7 shows the behavior during the first 50 s for the case in Fig. 6. The conditions emulate steady-state driving conditions at N = 2000 rpm and RL = 70% with E70 fuel. The target range of the ES controller (when it is activated) is an engine speed between 1900 rpm and 2100 rpm, and a relative load between 65% and 75%. At these conditions, the optimum spark timing has been identified through the conventional calibration process as $\theta_s^* = -19$ cad with corresponding combustion phasing CA50 of 10 cad.

In Figs. 6–8, subplot (a) shows the relative load RL (solid line) and the target load range (dashed lines). The ES controller state ξ, the spark timing θ_s, and the disturbance Δ in (5) are shown in subplot (b). The result of θ_s, the combustion phasing CA50 and the specific fuel consumption NSFC, is shown in subplots (c) and (d), respectively. The values of CA50 in subplot (c), and reported in the text, are always computed as an average over the combustion phasing in all the cylinders. In subplot (c) and (d), the raw data are shown together with the low-pass filtered data. In the experimental setup, the value of NSFC was calculated in the rapid prototyping system and was, therefore, not available when the controller is disabled. The ES controller is enabled except for the time marked by

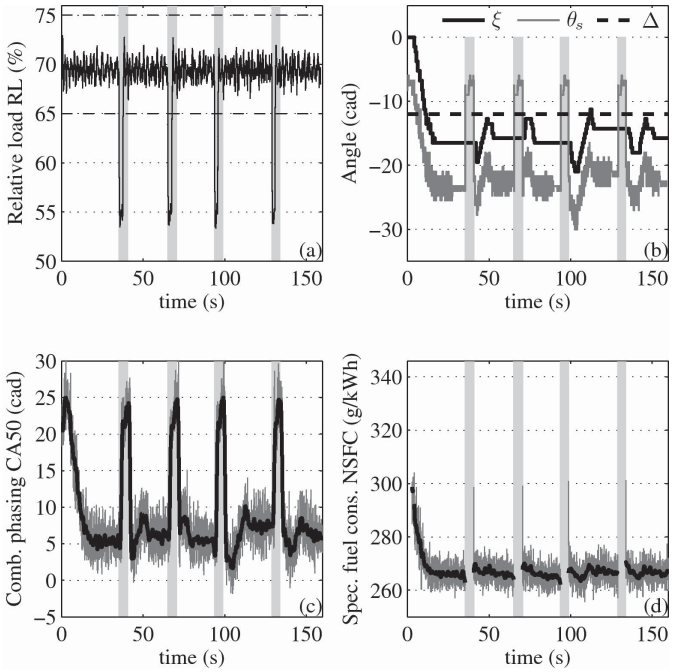

Fig. 6. ES controller performance for fixed load with a disturbance Δ of −12 cad from the optimum θ_s^*.

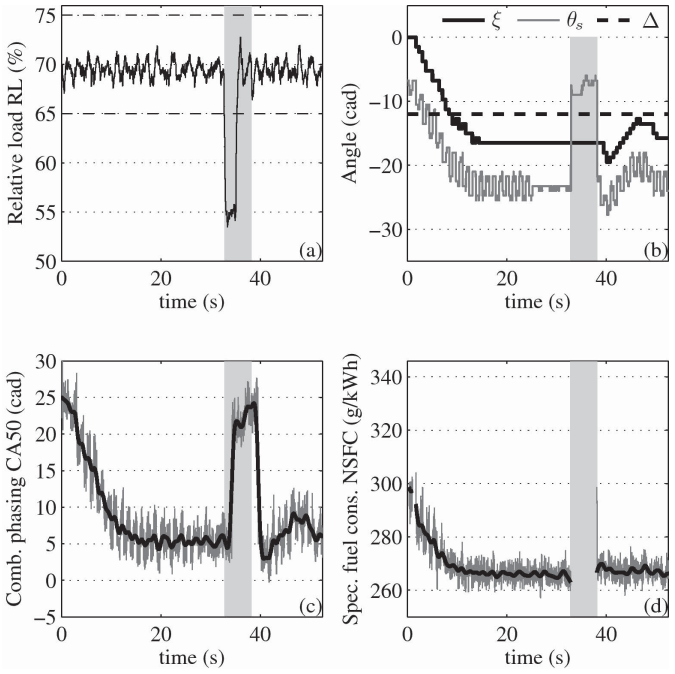

Fig. 7. Zoom of the first 50 s in Fig. 6 showing the ES controller performance for fixed load with $\Delta = -12$ cad.

gray areas in the plots. Recall from (6) that if $\xi = \Delta$ then the ES controller has perfectly canceled the artificially introduced disturbance Δ.

The test shown in Figs. 6 and 7 is initiated by retarding the spark from θ_s^* by $\Delta = -12$ cad so that the ECU map value $\tilde{\theta}_s$ is −7 cad. The load is perturbed, as described earlier, a while after convergence is detected such that the ES controller is disabled and then re-enabled. During these times, marked with

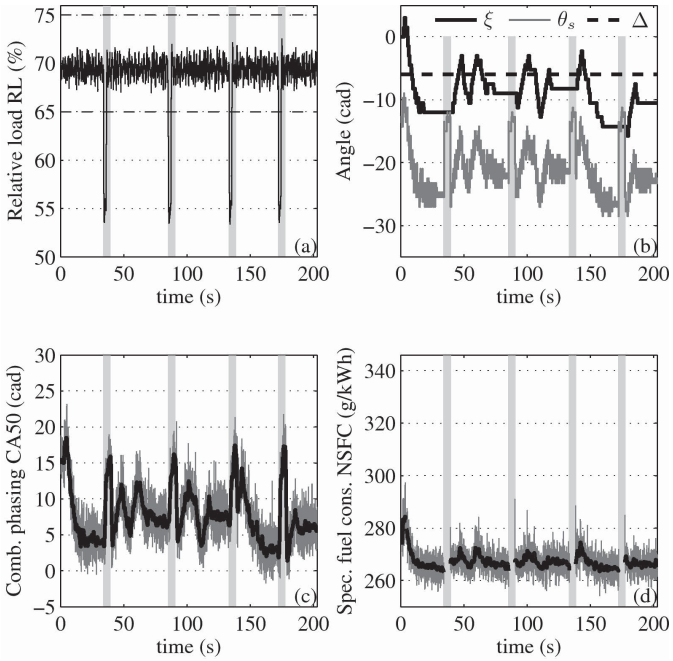

Fig. 8. ES controller performance for fixed load with a disturbance Δ of -6 cad from the optimum θ_s^*.

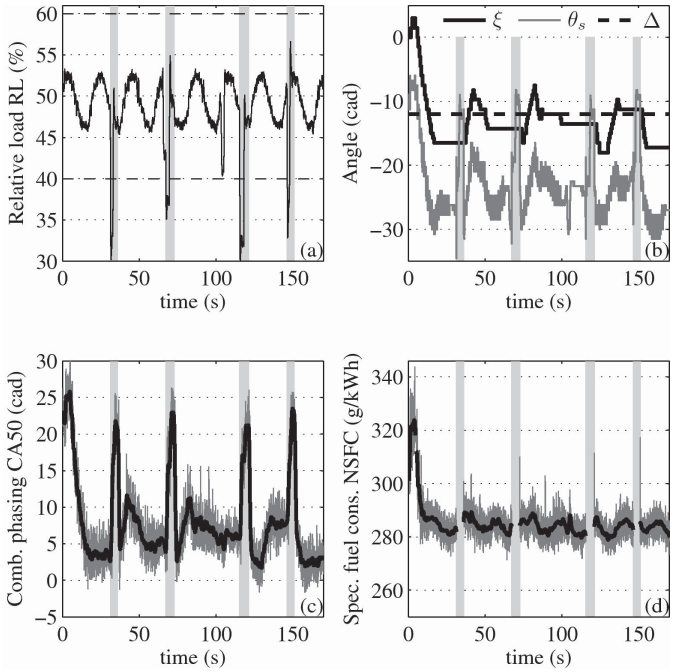

Fig. 9. ES controller performance for transient load with $A_L = 3\%$ and $T_L = 20$ s.

gray, the ES controller is disabled. In Fig. 6, the controller converges five times. The final values of θ_s are between -22 and -24 cad so the deviations from the pre-calibrated value in (6) are within -3 to -5 cad. Despite these deviations, the (filtered) NSFC values lie in between 265 and 266 g/kWh which are at the same level as for the pre-calibrated value. One can notice that the NSFC is fairly constant near the optimum spark timing, which correspond to the typically flat characteristics illustrated in Fig. 3. The average (and filtered) values of the combustion phasing are between 6 and 8 cad.

In the fixed load test shown in Fig. 8, the conditions are the same as earlier except for that the spark timing is retarded less aggressively with Δ being -6 cad. The deviations from the pre-calibrated value are slightly larger in this case, the final values of θ_s are between -21 and -26 cad, but the values of the NSFC are in between 265 and 266 g/kWh as before.

In summary, the tests show that it typically takes less than 20 s for the ES controller to reach steady state for these conditions. In addition, with the convergence criterion used here, 12 s of the steady state is required to detect convergence. Although the converged values for the spark timing were offset from the pre-calibrated value with up to 7 cad, the objective, NSFC, was approximately the same and between 265 and 266 g/kWh. Again, these results are justified due to the insensitivity of NSFC to θ_s close to the optimum demonstrated by the data from the spark sweep in Fig. 3. Finally, we note that similar convergence performance was observed in the other fixed load tests, given in Table II, with the same parameters in the ES controller.

C. Sinusoidal Load Commands

Transient experiments were performed by varying the commanded engine load according to (7) with the parameters in Table III. The fuel was E85. The performance for amplitudes A_L of 3% and 5% is similar and the results presented here are for A_L of 3% and varying T_L. It is assumed that the changes in NSFC due to these amplitudes for the varying load are small compared to the influence of the spark timing so that ES control is applicable inside the target range. As described in Section III, see Fig. 4, the commanded engine load is tracked by PI control of the throttle angle and the VVT is controlled by a calibration map in the ECU. Note that the air-fuel ratio is fixed at stoichiometry so the fuel mass is kept proportional to the inducted air mass. For the transient experiments, the nominal load was 50% and the engine speed was constant at 2000 rpm. The optimum spark angle θ_s^* for the nominal conditions is identified to be -23 cad. The target range is an engine speed between 1900 rpm and 2100 rpm and RL between 40% and 60%. The disturbance Δ in (5) was -12 cad for all these tests. The results are presented in Figs. 9 and 10 in an analogous manner to the previous section. Subplots (a), (c), and (d) show, respectively, the relative load RL, the combustion phasing CA50, and the specific fuel consumption NSFC. Subplot (b) shows the ES controller state ξ, the spark timing θ_s, and the disturbance Δ.

The results in Fig. 9 show the performance with amplitude A_L of 3% and period T_L of 20 s, superimposed on the nominal load of 50%, see (7). As before, the load was perturbed outside the target range after the controller converged, causing the controller to be disabled and then re-enabled. The ES controller reaches steady state rapidly in about 15 s during the first active period effectively advancing the combustion phasing CA50 from 22 cad to 4 cad. The obtained NSFC is about 284 g/kWh on average in the active periods, which is close to the pre-calibrated value. The time until steady state in less than 20 s for the other active periods except for the

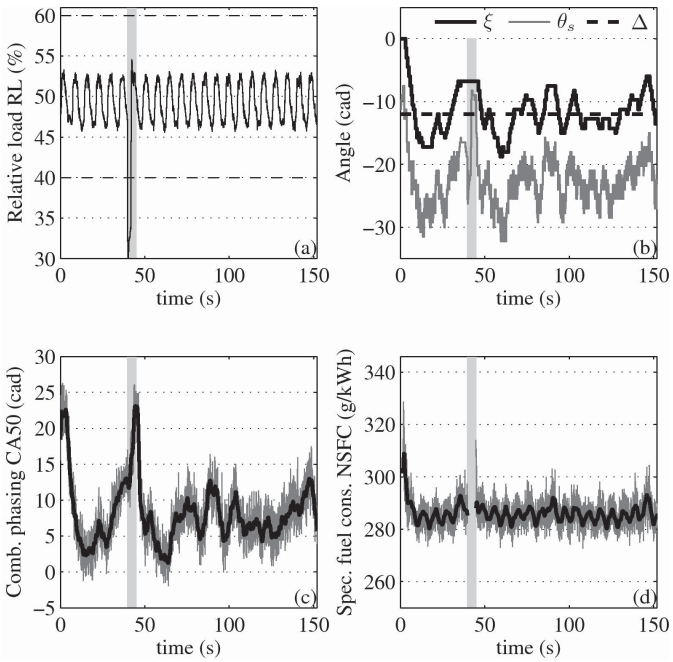

Fig. 10. ES controller performance for transient load with $A_L = 3\%$ and $T_L = 6.7$ s.

third period, starting at 70 s, where 25 s is required. The deviations, according to (6), at the end of each active period are between 1 and 5 cad, which are similar to the results with fixed load.

The conditions in Fig. 10 emulate transient driving conditions of a higher frequency, $T_L = 6.7$ s, with the same amplitude A_L of 3% RL as previously. The performance demonstrated previously in Fig. 9 was similar to the cases where T_L was 100 and 10 s. However, for $T_L = 6.7$ s, the load command changes so rapidly so that the ES controller only converges once at about 40 s during the duration of the experiment. However, note that the deviation (6) is maintained within $\pm$ 6 cad for 45 s and forward, which keeps the (filtered) NSFC in between 280 and 293 g/kWh. The average during the active periods is about 285 g/kWh (compared to 284 g/kWh in Fig. 9) and, hence, although the ES controller does not necessarily converge, the objective value, NSFC, is kept rather close the minimum value.

V. Conclusion

The complexity of a modern internal combustion engine makes the calibration a demanding process. With a flex-fuel engine, the complexity increases even further. To address these issues, an adaptive optimization scheme based on nonparametric extremum seeking was developed that manipulates the spark timing in order to maximize the fuel efficiency, which was estimated using cylinder pressure sensors. The air-fuel ratio was regulated to stoichiometry and the variations in spark timing are small; therefore, emissions after the three-way catalyst were not affected noticeably.

The performance of the ES controller was evaluated with experiments on a four-cylinder 2 L engine with both stationary and transient load conditions. In each experiment, the system was initialized with an offset from a known optimum that was determined prior to the experiments. For fixed load, the ES controller typically reaches steady state in 20 s with negligible deviation in the objective value, NSFC, compared to the known optimum. In the transients tests, where the commanded load is a biased sinusoid, similar performance is seen up to a sinusoid frequency of 0.1 Hz. When the load command is varying with a higher frequency, the results showed that although the ES controller may not reach steady state, the value of the NSFC is close to the optimum.

References

[1] A. G. Stefanopoulou, J. S. Freudenberg, and J. W. Grizzle, "Variable camshaft timing engine control," *IEEE Trans. Control Syst. Technol.*, vol. 8, no. 1, pp. 23–34, Jan. 2000.

[2] J. W. Grizzle, J. Buckland, and J. Sun, "Idle speed control of a direct injection spark ignition stratified charge engine," *Int. J. Robust Nonlin. Control*, vol. 11, no. 11, pp. 1043–1071, 2001.

[3] L. Eriksson, "Modeling and control of turbocharged SI and DI engines," *Oil Gas Sci. Technol., Rev. IFP*, vol. 62, no. 4, pp. 523–538, 2007.

[4] D. Lee, L. Jiang, H. Yilmaz, and A. G. Stefanopoulou, "Preliminary resluts on optimal variable valve timing and spark timing control via extremum seeking," in *Proc. IFAC Symp. Mechatron. Syst.*, 2010, pp. 377–384.

[5] D. Lee, L. Jiang, H. Yilmaz, and A. G. Stefanopoulou, "Air charge control for turbocharged spark ignition engines with internal exhaust gas recirculation," in *Proc. Amer. Control Conf.*, 2010, pp. 1471–1476.

[6] L. Jiang, J. Vanier, H. Yilmaz, and A. G. Stefanopoulou, "Parameterization and simulation for a turbocharged spark ignition direct injection engine with variable valve timing," in *Proc. SAE Congr.*, 2009, no. 2009-01-0680, 10.4271/2009-01-0680.

[7] D. Popovic, M. Jankovic, S. Magner, and A. R. Teel, "Extremum seeking methods for optimization of variable cam timing engine operation," *IEEE Trans. Control Syst. Technol.*, vol. 14, no. 3, pp. 398–407, May 2006.

[8] K. E. Shahroudi, "Robust design evolution and impact of in-cylinder pressure sensors to combustion control and optimization: A systems and strategy perspective," Ph.D. dissertation, Massachusetts Inst. Technol., Cambridge, MA, 2008.

[9] K. B. Ariyur and M. Krstić, "Wiley-Interscience publication," John Wiley & Sons, Inc., Hoboken, NJ, 2003.

[10] C. S. Draper and Y. T. Li, *Principles of Optimalizing Control Systems and an Application to the Internal Combustion Engine*. New York: ASME, 1951.

[11] J. Heywood, *Internal Combustion Engine Fundamentals*. New York: McGraw-Hill, 1988.

[12] P. F. Blackman, "Extremum-seeking Regulators," in *An Exposition of Adaptive Control*, J. H. Westcott, Ed. Pergamon Press, New York, 1962, pp. 36–50.

[13] A. C. Wakeman, J. M. Ironside, M. Holmes, S. I. Edwards, and D. Nutton, "Adaptive engine controls for fuel consumption and emissions reduction," in *Proc. Autom. Electron. Engine Manag. Driveline Controls Conf.*, 1987, pp. 870083–870087.

[14] M. Krstić and H. Wang, "Stability of extremum seeking feedback for general nonlinear dynamic systems," *Automatica*, vol. 36, no. 4, pp. 595–601, 2000.

[15] A. R. Teel and D. Popovic, "Solving smooth and nonsmooth multivariable extremum seeking problems by the methods of nonlinear programming," in *Proc. Amer. Control Conf.*, 2001, pp. 2394–2399.

[16] P. E. Wellstead and P. G. Scotson, "Self-tuning extremum control," *IEE Control Theory Appl., D*, vol. 137, no. 3, pp. 165–175, 1990.

[17] R. N. Banavar, "Extremum seeking loops with quadratic functions: Estimation and control," *Int. J. Control*, vol. 76, no. 14, pp. 1475–1482, 2003.

[18] P. G. Scotson and P. E. Wellstead, "Self-tuning optimization of spark ignition automotive engines," *IEEE Control Syst. Mag.*, vol. 10, no. 3, pp. 94–101, Mar. 1990.

[19] R. E. Dorey and G. Stuart, "Self-tuning control applied to the in-vehicle calibration of a spark ignition engine," in *Proc. 3rd IEEE Conf. Control Appl.*, Aug. 1994, pp. 121–126.

[20] S. Larsson and I. Andersson, "Self-optimising control of an Si-engine using a torque sensor," *Control Eng. Pract.*, vol. 16, no. 5, pp. 505–514, 2008.